Anion Binding of 1,1′-Bis(dialkylboryl)cobaltocenium Complexes − Structures of $[Co\{C_5H_4(BMe_2)\}_2]PF_6$, $Co[C_5H_4(BMe_2)][C_5H_4(BMe_2Cl)]$, $Co[C_5H_4(BiPr_2)]_2(\mu\text{-}F)$ and $NMe_4[Co\{C_5H_4(BiPr_2F)\}_2]$[‡]

Gerhard E. Herberich,*[a] Ulli Englert,[a] Andreas Fischer,[a][‡‡] and Dag Wiebelhaus[a][‡‡‡]

Keywords: Anion binding / Borates / Boron / Cobalt / Sandwich complexes

The cobaltocenium salts $[Co\{C_5H_4(BiPr_2)\}_2]PF_6$ [(**1a**)PF_6] and $[Co\{C_5H_4(BMe_2)\}_2]PF_6$ [(**1b**)PF_6] are strong Lewis acids. With pyridine (**1a**)PF_6 forms a mono-adduct **2** and a di-adduct **3** which show NMR spectra in the low-temperature regime of pyridine exchange. With chloride from PPh_4Cl the adduct formed is dynamic; quite remarkably, the formation of an anionic di-adduct is also observed. The mono-adducts (**1a**)X (X = F, Cl, Br, I, OH, and NH_2) and (**1b**)X (X = F, Cl, and OH) as well as the di-adduct salts $NMe_4[(\mathbf{1a})F_2]$ (**5**) and $K[(\mathbf{1a})(OH)_2]$ (**6**) are made by treating the salts (**1a**,**b**)PF_6 in CH_2Cl_2 or $MeNO_2$ with salts PPh_4X, NMe_4F, or powders of $NaNH_2$ or KOH in the appropriate ratios. X-ray single-crystal structures of the salt $[Co\{C_5H_4(BMe)_2\}_2]PF_6$ [(**1b**)PF_6], the semi-quaternized mono-adduct $Co[C_5H_4(BMe_2)][C_5H_4(BMe_2Cl)]$ (**4bd**) [B–Cl = 1.969(2) Å], the inverse chelate $Co[C_5H_4(BiPr_2)]_2(\mu\text{-}F)$ (**4ac**) with the very rare feature of fluorine bridging two boron centers [C_2 symmetric; B–F = 1.641(4) Å, B–F–B′ = 148.4(3)°], and the doubly quaternized di-adduct $NMe_4[Co\{C_5H_4(BiPr_2F)\}_2]$ (**5**) [exactly centrosymmetric; B–F = 1.477(4) Å] are given. Solution structures of the 1:1 products greatly depend on the nature of the anion, displaying i) exclusively ionic structures for (**1a**)PF_6 and (**1b**)PF_6, ii) semi-quaternized structures for the heavier halides (**1a**)Br (**4ae**) and (**1a**)I (**4af**) with some noticeable ionic dissociation, iii) semi-quaternized structures in equilibrium with minor amounts of inverse chelate isomers for (**1a**)F (**4ac**), (**1b**)Cl (**4bd**), and very likely for (**1a**)Cl (**4ad**), and iv) stable inverse chelate structures for $Co[C_5H_4(BiPr_2)]_2(\mu\text{-}NH_2)$ (**4aa**) (static in variable temperature NMR spectra, with diastereotopic Me groups), $Co[C_5H_4(BR_2)]_2(\mu\text{-}OH)$ [**4ab**: R = *i*Pr; **4bb**: R = Me; dynamic; for **4ab** T_c = 95 ± 5 °C, $\Delta G^{\neq}_{368}$ = 75(1) kJ·mol^{-1} for interchange of the diastereotopic Me groups], and $Co[C_5H_4(BMe_2)]_2(\mu\text{-}F)$ (**4bc**). The stability of the inverse chelates decreases in the order amide (**4aa**) > hydroxides (**4ab** and **4bb**) > fluorides (**4ac** and **4bc**) > chlorides (**4ad** and **4bd**), and also in the order BMe_2 > $BiPr_2$ (specifically **4bc** > **4ac**, and **4bd** > **4ad**). Variable temperature NMR spectra of solutions of **4bd** (CD_2Cl_2, 173–243 K) show that i) the ring-opening of the chelated chloride ($\Delta G^{\neq}_{368} \approx 45$ kJ·mol^{-1}) is energetically easier than for the chelated hydroxide **4ab**, ii) the predominance of the semi-quaternized isomer over the inverse chelate ($\Delta_R H$ = 2.5 ± 1.1 kJ·mol^{-1}, $\Delta_R S$ = 37.6 ± 5.4 kJ·mol^{-1}·K^{-1}) in the equilibrium is entropic in nature, and iii) the semi-quaternized isomer still undergoes fast chloride-exchange in the low-temperature regime of this equilibrium, proving the existence of an independent, intermolecular chloride-exchange mechanism.

Introduction

Anion recognition is one of the central themes of supramolecular chemistry,[3] and has been the subject of numerous reviews.[4] The binding of an anionic guest species to a host molecule may be caused mainly by one of three effects: electrostatic attraction by cationic centers, formation of polar bonds with Lewis-acidic centers, and formation of hydrogen bonds; these effects often act in combination.

The earliest example was the discovery in 1966, by Shriver and Biallas, that the 1,2-diborylethane $F_2BCH_2CH_2BF_2$ reacts with the trityl ether Ph_3COMe to give ether cleavage and formation of an inverse chelate $Ph_3C[(CH_2BF_2)_2(\mu\text{-}OMe)]$[5] with the anion being bonded simultaneously by two Lewis acid centers. Katz subsequently introduced 1,8-diborylnaphthalenes, which differ from the above-mentioned diborylethane in that they have their boron centers sterically fixed and thus are more close to the idea of a molecular pincer species.[6] This preorganization[7] of the chelating ligand ensures more efficient anion chelation since the reaction entropy is less unfavorable than in the case of the conformationally flexible 1,2-bis(difluoro-

[‡] Bis(boryl)metallocenes, 3; Part 2: Ref.[1] This work also forms part of a dissertation.[2]

[a] Institut für Anorganische Chemie, Technische Hochschule Aachen
52056 Aachen, Germany
Fax: +49-241-809-2288
E-mail: gerhard.herberich@ac.rwth-aachen.de
[‡‡] Current address: Grünenthal GmbH
Postfach 50 04 44, 52099 Aachen, Germany
[‡‡‡] Current address: BASF AG, Competence Center Global Purchasing, GR/S
Benckieserplatz 1 − BZM1, 67056 Ludwigshafen, Germany

boryl)ethane. Conformationally rigid chelate ligands have also been made by other groups[8] and have recently been used for the construction of highly electrophilic anion pincers.[9]

In this paper we treat anion binding by cationic two-boron host species, the two 1,1′-bis(dialkylboryl)cobaltocenium cations **1a**$^+$ and **1b**$^+$, in the form of their hexafluorophosphate salts. These cationic anion pincers possess a skeletal flexibility similar to that of a diborylethane, but in contrast to the older two-boron examples, they are cationic and exert an electrostatic field effect which adds stability to their anion complexes.

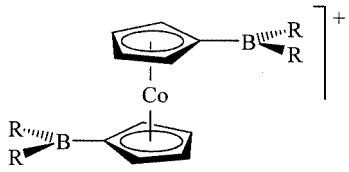

1a$^+$: R = *i*Pr; **1b**$^+$: R = Me

Cations of type **1** give rise to strong cation-anion interactions, and four structural types are encountered: type **A** with purely ionic interactions, a semi-quaternized type **B** with a zwitterionic situation, type **C** with an inverse chelate structure, and finally the doubly quaternized type **D**. In our preliminary communication of this topic we have already described one example each of types **A**−**C** [the compounds (**1a**)PF_6, (**1a**)Cl, and (**1a**)(OH), respectively],[10] while an example of type **D** structures will be given below for the first time.

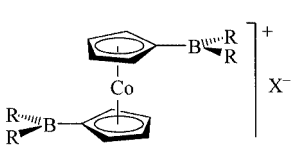

A

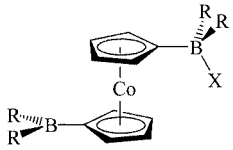

B

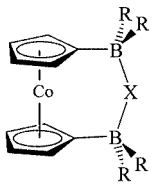

C

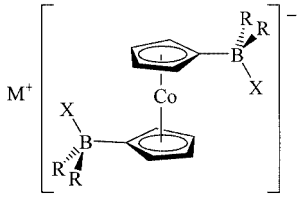

D

Before becoming more specific we note a detail of great analytical value. The pincer cation **1a** with the diisopropylboryl substituents will have diastereotopic methyl groups in the structures of type **C** and **D** and for one of the ligands of type **B**, provided these structures are not dynamic. In all other cases the methyl groups are equivalent. This feature will provide us with insights which remain hidden in case of the dimethylboryl analogue **1b**$^+$.

Results and Discussion

Synthesis of the Anion Binding Cobaltocenium Ions

The diisopropylboryl compound (**1a**)PF_6 can be made in a straightforward two-step synthesis.[10] First, the cobaltocene **1a** is prepared from Li[C_5H_4(B*i*Pr$_2$)][11]/$CoBr_2$(DME). Subsequent oxidation with [$FeCp_2$]PF_6 [12] in dichloromethane affords the desired compound, which was characterized structurally as an ionic compound without specific cation-anion interactions.

The dimethylboryl analogue (**1b**)PF_6 could potentially be made by an analogous sequence. For practical reasons it seemed more convenient to synthesize it by a different route. First we prepared the cobaltocene Co[C_5H_4-{B(NEt_2)$_2$}]$_2$ and, by quantitative oxidation with C_2Cl_6, the corresponding chloride [Co{C_5H_4[B(NEt_2)$_2$]}$_2$]Cl.[1] Subsequent treatment with BCl_3 and then with Al_2Me_6 afforded the salt (**1b**)$AlCl_4$, and, by anion metathesis, (**1b**)PF_6.[1]

First Observations

In a first series of NMR-tube experiments a solution of (**1a**)PF_6 in CD_2Cl_2 was treated with varying amounts of pyridine. Formation of a mono-adduct **2** and of a di-adduct **3** was observed, quite as expected. If the ratio of the reactants py/**1a**$^+$ is chosen close to 1:1 or to 2:1 the respective adducts can be isolated by crystallization at −30 °C; they were not characterized in detail.

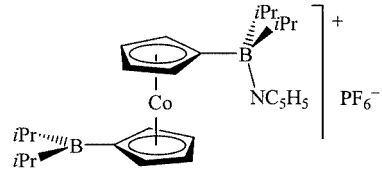

2

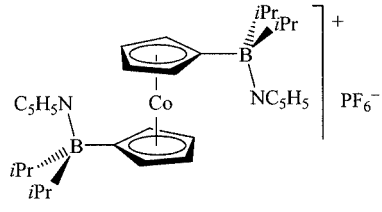

3

Several observations are of interest. First, the reaction mixtures are close to the slow-exchange regime, and all species involved can be observed separately in the ^1H, ^{13}C, and ^{11}B NMR spectra. However, the hyperfine structure of the ring protons is blurred and the two different rings of **2** cannot be distinguished in the $^1H\{^1H\}$ NOE difference

spectrum, indicating a slow exchange of the pyridine. The adduct-formation equilibria are far on the right side as no free pyridine is seen at py/**1a**$^+$ ratios below two. Also, the adduct formation to give **3** is less strong than the formation of **2** as no di-adduct **3** is seen at py/**1a**$^+$ ratios lower than one. These observations are remarkable since the pyridine adducts of the known uncharged complexes $M(CO)_2\{C_5H_4(BMe_2)\}$ (M = Co, Rh) show fast exchange with excess pyridine.[13] Hence the cation **1a**$^+$ is a comparatively stronger Lewis acid, even in the second stage.

In a second experiment we titrated (**1a**)PF_6 with PPh_4Cl in dichloromethane solution and monitored the ensuing reaction by ^{11}B NMR spectroscopy (Figure 1). Only one ^{11}B NMR signal is seen over the entire range of the titration, indicating a fast-exchange regime for the interaction of cation **1a**$^+$ and Cl^-.

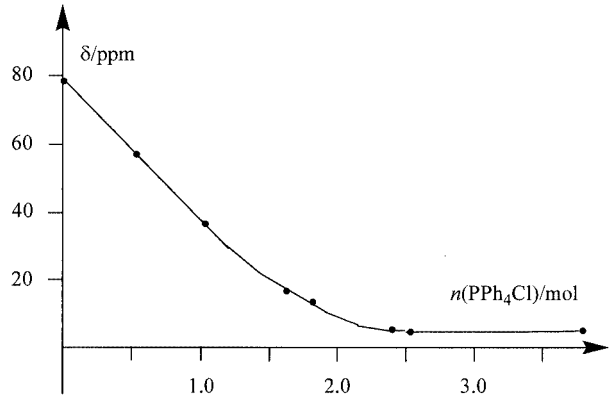

Figure 1. Boron chemical shifts during titration of (**1a**)PF_6 with PPh_4Cl in CD_2Cl_2

The chemical shift at the beginning of the titration (δ = 79 ppm) is that of **1a**$^+$ and conforms to the expected value for dialkylarylboranes, while the final chemical shift (δ = 5 ppm) indicates the presence of a fully quaternized species, the anionic species $[(\mathbf{1a})Cl_2]^-$.[14] The first addition of Cl^- to **1a**$^+$ is energetically rather favorable since we observe a straight line for the chemical-shift values up to a ratio of $Cl^-/\mathbf{1a}^+ \leq 1$. The product (**1a**)Cl is dynamic and shows a chemical shift (δ = 37 ppm) which can be understood as the mean of the chemical shifts for one trigonal and one tetrahedral boron center. Hence, the product (**1a**)Cl possesses the same semi-quaternized structure in solution that has also been found in the crystal.[10] The second addition of Cl^- is less favorable energetically, as indicated by the curvature of the line, and an excess of Cl^- (almost 2.5 mol) is needed to complete the formation of $PPh_4[(\mathbf{1a})Cl_2]$, the doubly quaternized end-product. Below we shall discuss the nature of the observed chloride-exchange process for (**1a**)Cl and also give a more thorough comment on its solution structure.

Synthetic Methods I: Uncharged Complexes

Complexes of types **B** and **C** were made by essentially the same general method. We treated the salts (**1a**,**b**)PF_6 in CH_2Cl_2, or occasionally in nitromethane, with a second salt such as NMe_4F, PPh_4Cl, PPh_4Br, and PPh_4I in a 1:1 ratio. The large organic cations ensured a sufficient solubility. If such salts were not readily available, inorganic salts such as KOH and $NaNH_2$ had to be used in powdered form, and long reaction times were required. After completion of the reaction the polar solvent was removed. The product was then extracted with toluene and isolated from that solvent. When crystals were desired the material was recrystallized from CH_2Cl_2/toluene. Yields were mostly very good, but no reactions were achieved with NMe_2^-, OMe^-, and OPh^-, and attempted addition of hydride induced decomposition. In some cases oxidation of the cobaltocene **1a** could be used as an alternative method, and (**1a**)Cl (**4ad**) and (**1a**)(OH) (**4ab**) were made in this way (Scheme 1).[10]

$$[Co\{C_5H_4(BR_2)\}_2]PF_6 \xrightarrow[-ZPF_6]{+ZX} Co[C_5H_4(BR_2)]_2 * X$$

(**1a**,**b**)PF_6 — **4**

Z = NMe_4, PPh_4

4, R = *i*Pr	**aa**	**ab**	**ac**	**ad**	**ae**	**af**
R = Me		**bb**	**bc**	**bd**		
X	NH_2	OH	F	Cl	Br	I

Scheme 1

Synthetic Methods II: Doubly Quaternized Complexes

The salt $PPh_4[(\mathbf{1a})Cl_2]$ that was observed in the titration experiment was not stable enough to be isolated. However, with the more Lewis basic anions F^- and OH^- salts with doubly quaternized anionic complexes could be isolated. When (**1a**)PF_6 in CH_2Cl_2 was treated with NMe_4F in a 1:2 ratio, the ammonium fluoride dissolved despite its low solubility in that solvent (Scheme 2). Since the resulting robust product $NMe_4[(\mathbf{1a})F_2]$ (**5**) readily dissolves in toluene it can be isolated by the same general technique described above. It was crystallized by slowly concentrating its solution in toluene or by recrystallization from CH_2Cl_2/Et_2O. The analogous treatment of (**1a**)PF_6 in CH_2Cl_2 with an excess of finely ground KOH afforded the potassium salt $K[(\mathbf{1a})(OH)_2]$ (**6**), which can be crystallized from toluene/hexane. Treatment of the hydroxide **4ab** with KOH also produces complex **6**. The conceivable alternative of a deprotonation is not observed.

$$[Co\{C_5H_4(BiPr_2)\}_2]PF_6 \xrightarrow[-ZPF_6]{+2\,ZX} Z[Co\{C_5H_4(BiPr_2X)\}_2]$$

(**1a**)PF_6 — **5**: Z = NMe_4, X = F; **6**: Z = K, X = OH

Scheme 2

Crystal Structures of (1b)PF_6, 4bd, 4ac, and 5

We present four crystal structures which exemplify the four archetypal cation-anion interactions (**A**−**D**) mentioned

above. Compound (**1b**)PF_6 is ionic with essentially purely electrostatic interaction between the anion and **1b**$^+$ (type **A**; Figure 2). The chloride **4bd** displays a semi-quaternized structure (type **B**; Figure 3). For **4ac** an inverse chelate type is observed (type **C**; Figure 4), and **5** finally has a doubly quaternized structure (type **D**; Figure 5).

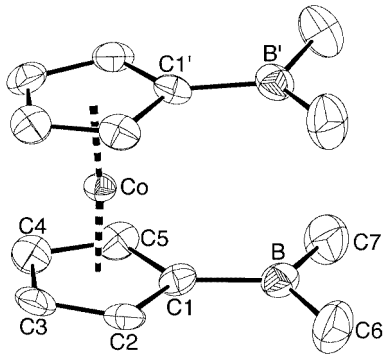

Figure 2. Structure of the cation of (**1b**)PF_6 (PLATON plot[15] at the 50% probability level); selected bond lengths (Å): Co−C 2.032 (av.) [range 2.021(3)−2.055(4)], C1−B 1.566(6), C6−B 1.554(6), C7−B 1.542(7)

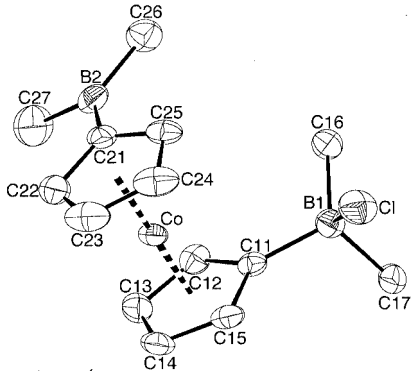

Figure 3. Structure of the chloride **4bd** (PLATON plot[15] at the 50% probability level); selected bond lengths (Å): Co−C(Cp1) 2.034 (av.) [with one long bond Co−C11 2.074(2)], B1−Cl 1.968(2), C11−B1 1.614(3), C16−B1 1.628(3), C17−B1 1.654(3), Co−C(Cp2) 2.038 (av.) [range 2.027(2)−2.044(2)], C21−B2 1.567(3), C26−B2 1.551(3), C27−B2 1.563(3)

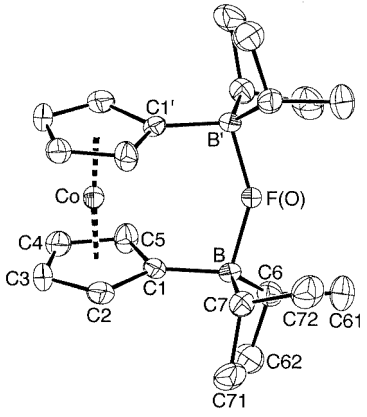

Figure 4. Structure of the inverse chelate **4ac** (PLATON plot[15] at the 50% probability level); selected bond lengths (Å) and angles (°): Co− C 2.023 (av.) [range 2.012(3) − 2.033(3)], B−F 1.641(4), C1−B 1.629(4), C6−B 1.606(5), C7−B 1.620(5), F(O)−H 0.9390(19); B−F−B′ 148.4(3), B−F(O)−H 105.80(13)

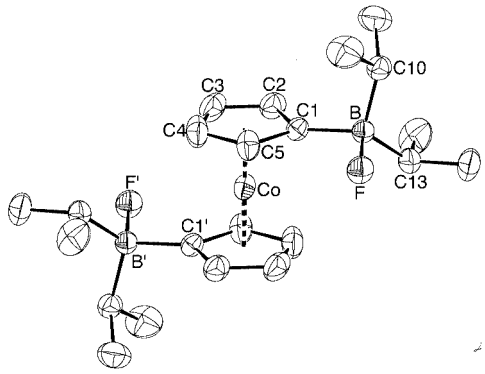

Figure 5. Structure of the anion of **5** (PLATON plot[15] at the 30% probability level); selected bond lengths (Å): Co−C1 2.095(3), Co−C2 2.022(4), Co−C3 2.007(4), Co−C4 2.018(4), Co−C5 2.031(3), B−F 1.478(3), C1−B 1.627(4), C10−B 1.634(4), C13−B 1.626(4)

All structures contain a cobaltocenium moiety with the usual metal−ring distance for formal cobalt(III) (close to 1.63 Å), regardless of its actual overall charge. The salt (**1b**)PF_6 displays crystallographic mirror symmetry and hence an exactly eclipsed conformation. The resulting transannular repulsion is reflected in a ring tilt of 6.3(2)°; all other structures contain parallel planar ring systems. The torsion angle (B−cog-cog′−B′)[16] varies from exactly 0° for (**1b**)PF_6 through 26° for **4ac** and 83° for **4bd** to exactly 180° for **5**. This last compound displays crystallographic centrosymmetry which places the two negative charge centers of the anion $[Co\{C_5H_4(BiPr_2F)\}_2]^-$ at maximum distance. In all other cases the ring-ring torsional mode should be very soft, and the torsional angle observed should largely be determined by lattice forces.

Next we consider the distance B···B′. This distance is 3.543(7) Å in the structure of (**1b**)PF_6, and would be 3.270 Å for the same cation with parallel eclipsed rings. In the inverse chelate $Co[C_5H_4(BF_2)]_2(\mu\text{-}OH)$ it amounts to only 2.752(4) Å,[1] demonstrating a variation of the B···B′ distance of up to 0.8 Å for eclipsed conformations. Ring-ring rotation adds further variability to the pincer bite of the cations **1a**,**b**$^+$.

Of general interest are the boron−anion distances as they should be related qualitatively to the strength of the cation−anion interaction. Bond lengths for chlorine fixed to a quaternized boron center vary within a wide range of 1.76 to 1.92 Å.[17] The average value is about 1.83 Å[18] and distances at the higher end of the given range are considered as weak.[17a] We should, however, remember in this context that the sizeable electrostatic contribution to the bonding interaction varies roughly with 1/*r* and thus is only weakly affected by small bond-length variations. The B−Cl distance for the *B*-methyl compound **4bd** is even longer, with a value of 1.969(2) Å. The same distance in the *B*-*i*Pr compound **4ad** [1.982(3) Å] is marginally longer;[10] a marked steric influence of the isopropyl groups is not seen here.

The reported B−F bond lengths (for bonds with terminal fluorine) lie in a comparatively narrow range from 1.36 to 1.43 Å for quaternized boron centers.[19] All of these dis-

tances are from compounds with more than one fluorine atom directly attached to boron. Substitution of fluorine with an alkyl substituent leads to less-positive boron centers and, consequently, to longer distances for the remaining B−F bonds. Thus, for BF_4^- an average of 1.37 Å has been found,[18] whereas for $MeBF_3^-$ a value of 1.424 Å has been reported.[19e] Therefore the observed value of 1.477(4) Å for **5** seems to conform to expectations for a fluorotriorganoborate.

Before discussing the B−F distance in **4ac**, we have to consider the identity of the material isolated as **4ac**. In our previous work an attempted synthesis of $Co[C_5H_4(BF_2)]_2(\mu\text{-}F)$ resulted in the isolation of $Co[C_5H_4(BF_2)]_2(\mu\text{-}OH)$,[1] thus indicating a strong preference for OH^- binding of the corresponding pincer cation. In the present case, the ^1H NMR spectra showed the presence of small admixtures of the hydroxo compound **4ab** which increased when the material was manipulated, for instance in a recrystallization procedure. The structural data for **4ac** are very similar to those reported for **4ab**,[10] showing the same space group (*Pccn* no. 56), the same crystallographic C_2 symmetry of the inverse chelate, and rather similar atomic coordinates, bond lengths, and angles. These observations suggested that the two compounds might cocrystallize; hence the structure was refined assuming cocrystallization of **4ac** and **4ab**. The refinement converged for a **4ac/4ab** ratio of 79(3)/21(3). Thus, a high predominance of the fluoride **4ac** in the crystal picked for the structure determination can be considered as certain.

The structure of the inverse chelate **4ac** is highly unusual in that it displays a fluorine bridging two boron centers. A search in the Cambridge Structural Database (CSD)[20,21] resulted in only two hits, a structure with the heptafluorodiborate ion $B_2F_7^-$ [B−F = 1.50(1) and 1.51(1) Å with B−F−B = 128.1(7)°],[22] and the structure of 9-fluoro-9-borabicyclo[3.3.1]nonane, which displays an unsymmetrical self-association with a long bond between a tetracoordinate boron center and a bridging fluorine [B−F = 1.652(5) Å].[23] For the inverse chelate **4ac** the B−F bond length [1.641(4) Å] is, not surprisingly, longer than in $B_2F_7^-$ and similar to that of the comparable bond of 9-fluoro-9-borabicyclo[3.3.1]nonane**.** The bond angle around the bridging fluorine of 148.4(3)° seems remarkably large; a shift of the fluorine atom toward the cobalt center decreases the transannular repulsion of the two B*i*Pr$_2$ groups (for evidence of this repulsion see below) and increases the electrostatic attraction between the negative fluorine and the positive metallocenium region of **4ac**.

Structure in Solution I

Boron chemical shifts give first indications as to which structures exist in solution. Figure 6 gives an overview over the chemical-shift values observed. Three regions may be distinguished. At the high (left) end of the scale the salts (**1a**,**b**)PF_6 mark the position of the "naked" trigonal boron (δ = 78 ppm). At the low end are the inverse chelate molecules (δ = 1.4 to −8.5 ppm) with exclusively tetrahedral boron centers which, in fact, display their signal in the same region as the doubly quaternized salts **5** and **6**. In the central region the chlorides **4ad** and **4bd** mark the region of the semi-quaternized molecules (δ = 37 ppm) with a mean chemical shift for one trigonal (δ = 78 ppm) and one tetrahedral boron (roughly δ = 0 ppm). The higher chemical-shift values for the bromide **4ae** and even more so for the iodide **4af** indicate that there is more tricoordinate boron than tetracoordinate boron, in other words, that there is a dissociation equilibrium (Scheme 3). Finally, while the fluoride **4bc** fits the overall picture, the sterically more crowded diisopropylboryl analogue **4ac** shows an anomalously high chemical shift which will be discussed further below.

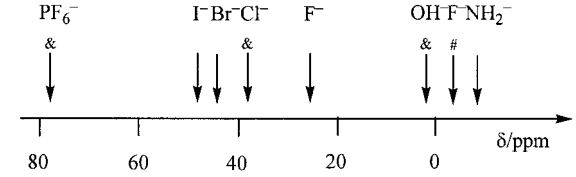

Figure 6. Boron chemical shifts of the combinations (**1a**)PF_6/X^-; &: the related combination (**1b**)PF_6/X^- shows the same chemical shift; #: the signal for (**1b**)PF_6/F^- appears at higher field

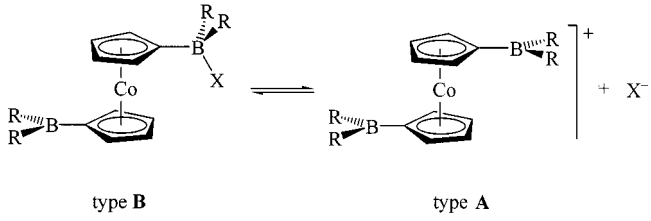

R = *i*Pr, Me; X = Cl−, Br−, I−

Scheme 3

Structure in Solution II: Inverse Chelates

The inverse chelate complexes **4aa**, **4ab**, and **4ac** possess two types of diastereotopic methyl groups (within their B*i*Pr$_2$ groups) which should give rise to two doublets in the ^1H NMR spectra. In the case of the rather stable hydroxide **4ab**[10] these two doublets are seen at ambient temperature. However, when a solution of **4ab** in $C_2D_2Cl_4$ is warmed up, line-broadening sets in at 60 °C. Despite the onset of decomposition fast measurements give a coalescence temperature, T_c, of 95 ± 5 °C which corresponds to a barrier $\Delta G^{\neq}_{368}$ of 75(1) kJ·mol^{-1}. The underlying dynamic process must imply ring-opening of the chelate and rotation of a diisopropylboryl group. In the case of the robust amide **4aa** the doublets are sharp even at 115 °C. Thus the chelate structure of the amide is more stable than that of the hydroxide. On the other hand, the fluoride **4ac** is already dynamic at ambient temperature, showing only one doublet. These observations show that the stability of the inverse

chelate forms increases in the order fluoride **4ac** < hydroxide **4ab** < amide **4aa**.

The anomalously high chemical shift for **4ac** mentioned above indicates a fast equilibrium between the semi-quaternized form **4ac-B** and the chelate form **4ac-C** (Scheme 4). We may take the shift of the methyl compound **4bc** (δ = −2.5 ppm) as representative of the chelate form **4ac-C**, and estimate a 65% contribution of the open form **4ac-B** to the equilibrium mixture (NMR tube, ambient temperature). Furthermore, the comparison of **4ac** and **4bc** proves that the sterically more demanding isopropyl groups effect a marked destabilization of the chelate structure **C**.

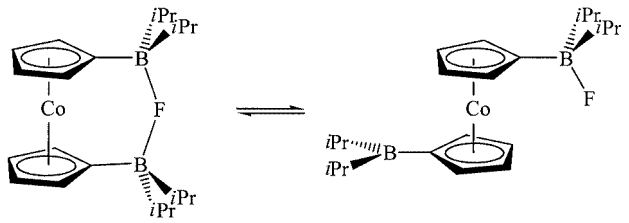

4ac-C **4ac-B**

Scheme 4

Structure in Solution III: The Chlorides 4ad and 4bd

A more direct observation of the equilibrium between semi-quaternized form **B** and chelate form **C** (cf. Scheme 4) seemed desirable. Variable temperature NMR spectra (173−243 K) of the chloride **4bd** in CD_2Cl_2 solutions revealed that this chloride may also form a chelate isomer (Scheme 5). The exchange reaction is slow below 200 K, and the chelate isomer contributes 5−7% to the equilibrium mixture. Note in this context that a chloride bridging two boron centers has previously been observed in the structurally characterized compound $(Ph_3PNPPh_3)[1,8\text{-}C_{10}H_6(BCl_2)_2(\mu\text{-}Cl)]$ derived from the rigid pincer molecule 1,8-bis(dichloroboryl)naphthalene.[6c]

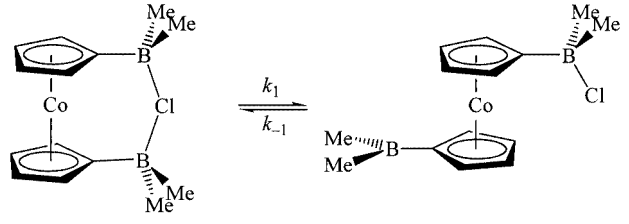

4bc-C **4bc-B**

Scheme 5

The equilibrium is close to thermoneutral ($\Delta_R H$ = 2.5 ± 1.1 kJ·mol^{-1}), showing that the bond strength for the bridging B−Cl bond is about half that of the terminal B−Cl bond. Ring-opening of the chelate **4bd-C** is endotropic ($\Delta_R S$ = 37.6 ± 5.4 kJ·mol^{-1}·K^{-1}), and the equilibrium is entropy driven in the accessible temperature range. The sign of the reaction enthalpy suggests, though with only moderate significance, that the major isomer **4bd-B** does not represent the ground-state isomer.

Line-shape analysis (^{1}H and ^{13}C NMR, 193−243 K) with the help of the program D NMR-SIM[24] provided rate constants, and from these activation parameters.[25] The estimated free enthalpy of activation for the ring-opening of **4bd-C** is estimated to be about 45 kJ·mol^{-1}, much less than in the case of the hydroxide **4ab** discussed above, as expected.

The low-temperature NMR spectra hold another surprise: the major isomer **4bd-B**, quite unexpectedly, shows only a single ligand pattern of effective C_{2v} symmetry. Since we do see separate spectra for the two isomers, the *intra*molecular chloride exchange implied in Scheme 5 is frozen out at 200 K. What is still possible is an *inter*molecular chloride-exchange mechanism with the chloride migrating from the boron in one open molecule **4bd-B** to the next one. Several detailed mechanisms are conceivable; for instance, a dissociation with formation of $\mathbf{1b}^+$ and free Cl^- analogous to Scheme 3 and subsequent chloride transfer between **4bd-B** and the trace cation $\mathbf{1b}^+$ is a likely possibility.

In the case of the chloride **4ad** variable temprature NMR spectra revealed line-broadening in an intermediate temperature range (as for **4bd**), but no chelate isomer **4ad-C** could be detected in the low-temperature regime (< 200 K). This seemingly puzzling situation can now easily be understood. From what we have seen in the fluoride cases we should expect that the contribution of the chelate form **4ad-C** is smaller than for the methyl compound **4bd**. Experimentally it is obviously below the level of detection (< 2%), but the line-broadening still observed is again evidence of a dynamic process, most likely analogous to that of Scheme 5.

Concluding Remarks

The chelating properties of pincer molecules may be influenced (inter alia) by preorganization of the coordinating centers and by field effects. The pincer cations $\mathbf{1a,b}^+$ allow ring-ring rotation, and thus have little preorganization, but they possess a positive charge which favors anion binding. Three features are particularly noteworthy: formation of Lewis base adducts in the slow-exchange regime (with pyridine), formation of anionic di-adducts with anions (with F^-, OH^-, and in solution with Cl^-), and formation of inverse chelates with monoatomic anions, surprisingly including F^-. In summary, our observations strongly underline the favorable effect of the positive charge on the anion binding properties of pincer cations such as $\mathbf{1a,b}^+$.

Experimental Section

General Remarks: Reactions were carried out under an atmosphere of dinitrogen by means of conventional Schlenk techniques. Hexane was distilled from potassium, THF from sodium benzophenone ketyl, dichloromethane from calcium hydride and nitromethane was condensed after passing through a column of acti-

vated alumina. Silica and alumina were heated under vacuum at 300 °C and kept under dinitrogen.

KOH was prepared from KH and water in THF. $NaNH_2$ was bought as a suspension in xylene, washed with hexane and dried under vacuum to yield a grey powder. NMe_4F was bought from Acros; all other reagents were from Aldrich and were used without purification.

NMR spectra were recorded on a Varian Unity 500 spectrometer (^{1}H: 500 MHz; ^{13}C: 125.7 MHz), a Varian VXR 300 (^{1}H: 300 MHz; ^{13}C: 75.4 MHz), Bruker WM-250 FT (^{1}H: 250 MHz; ^{13}C: 62.9 MHz) or a Rototec/Piccinotti Mini-FID (^{11}B: 29 MHz) and calibrated using referenced solvent signals. Mass spectra were recorded on a Finningan MAT-95 spectrometer. Elemental analyses were determined by the Analytische Laboratorien Malissa and Reuter, Lindlar, Germany.

Pyridine Adducts 2 and 3: A solution of (**1a**)PF_6 in CD_2Cl_2 was treated with defined successive portions of pyridine (from 0.7 to 2.2 equivalents). After each addition NMR spectra were recorded.
2: ^{1}H NMR (500 MHz, CD_2Cl_2): δ = 0.52 and 0.63 (d, $^3J \approx$ 6.8 Hz, 2 × 6 H, 2 Me′ each), 1.15 (d, ^3J = 7.3 Hz, 4 Me), 1.23 (sept, ^3J = 7.3 Hz, 2 BCH′), 1.99 (sept, ^3J = 7.3 Hz, 2 BCH), 5.20 (br. s, 2-/5-H′), 5.51 (br. s, 3-/4-H′), 5.84 (br. s, 2-/5-H), 5.95 (br. s, 3-/4-H), 7.91 (m, 2 H_m), 8.25 (m, H_p), 8.76 (m, 2 H_o) ppm. ^{11}B{^{1}H} NMR (160 MHz, CD_2Cl_2): δ = 78.7, 2.0 ppm. ^{13}C{^{1}H} NMR (126 MHz, CD_2Cl_2): δ = 18.5 (br., BCH′), 18.66 (Me), 18.94 and 19.99 (Me′), 23.26 (br., BCH), 82.08 (C-2′,5′), 87.13 (C-3′,4′), 89.91 (C-2,5), 90.27 (C-3,4) ppm; pyridine: δ = 126.58 (C-3,5), 141.92 (C-4), 145.86 (C-2,6) ppm.
3: ^{1}H NMR (500 MHz, CD_2Cl_2): δ = 0.58 and 0.65 (br. d, $^3J \approx$ 7.0 Hz, 2 × 12 H, 4 Me each), 1.26 (sept, 4 BCH), 5.18 (m, 2 2-/5-H), 5.60 (m, $N = {}^3J_{2,3} + {}^4J_{2,4}$ = 3.7 Hz, 2-/3-/4-H), 7.83 (m, 4 H_m), 8.22 (m, 2 H_p), 8.82 (m, 4 H_o) ppm. ^{11}B{^{1}H} NMR (160 MHz, CD_2Cl_2): δ = 2.3 ppm. ^{13}C{^{1}H} NMR (126 MHz, CD_2Cl_2): δ = 18.7 (br., BCH), 19.17 and 20.18 (Me), 83.76 (C-3,4), 86.70 (C-2,5) ppm; pyridine: δ = 126.28 (C-3,5), 141.70 (C-4), 146.02 (C-2,6) ppm.

Co[C_5H_4(B*i*Pr$_2$)]$_2$(μ-F) (4ac): Solid NMe_4F (206.5 mg, 2.22 mmol) was added with stirring to a solution of (**1a**)PF_6 (1.17 g, 2.22 mmol) in CD_2Cl_2 (20 mL) at room temperature. After 30 minutes all volatiles were removed under vacuum. The yellow powdery residue was transferred to a frit and extracted with toluene until the filtrate remained colorless. The combined solutions were freed from solvent to give the product **4ac** (428.3 mg, 49%) as a yellow microcrystalline solid, m.p. 127 °C (dec.); the product always contained an admixture of the hydroxy compound **4ab**. $C_{22}H_{36}B_2CoF$ (400.1) calcd. C 66.05, H 9.07; found C 66.35, H 9.32. SIMS (K/T): positive ions *m*/*z* (%) = 381 (100) [M^+ − F], 357 (31) [M^+ − *i*Pr]; negative ions *m*/*z* (%) = 400 (100) [M^-], 357 (17) [M^- − *i*Pr], 137 (23) [C_5H_4B*i*PrF$^-$], 65 (35) [Cp^-]. ^{1}H NMR (500 MHz, CD_2Cl_2): δ = 0.92 (d, ^3J = 7.3 Hz, 8 Me), 1.15 (sept, ^3J = 7.3 Hz, 4 BCH), 5.40 (m, 2 C_5H_4) ppm. ^{11}B{^{1}H} NMR (160 MHz, CD_2Cl_2): δ = 26.4 ppm. ^{13}C{^{1}H} NMR (126 MHz, CD_2Cl_2): δ = 20.50 (Me), 21.6 (br., BCH), 83.68 (C-3,4), 87.92 (C-2,5) ppm. ^{19}F NMR (470 MHz, C_6D_6): δ = −158 ($\nu_{1/2}$ = 207 Hz).

Co[C_5H_4(BMe$_2$)]$_2$(μ-F) (4bc): A preparation as described for (**1a**)F from NMe_4F (58.2 mg, 0.410 mmol) and (**1b**)PF_6 (171.0 mg, 0.413 mmol) gave **4bc** (113.0 mg, 96%) as a yellow powder which could be recrystallized from toluene/CD_2Cl_2. SIMS (DTE/DTT/Sul): positive ions *m*/*z* (%) = 269 (100) [M^+ − F], 229 (64) [CoCp{C_5H_4(BMe$_2$)}$^+$]. ^{1}H NMR (250 MHz, CD_2Cl_2): δ = −0.10 (s, 4 Me), 5.19 (m, 2 2-/5-H), 5.25 (m, N = 3.7 Hz, 2 3-/4-H) ppm. ^{11}B{^{1}H} NMR (29 MHz, CD_2Cl_2): δ = −2.5 ppm. ^{13}C{^{1}H} NMR (63 MHz, CD_2Cl_2): δ = 11.5 (br., Me), 82.79 (C-3,4), 87.45 (C-2,5) ppm.

Co[C_5H_4(B*i*Pr$_2$)][C_5H_4(B*i*Pr$_2$Cl)] (4ad): Solutions of (**1a**)PF_6 (281.7 mg, 0.536 mmol) and PPh_4Cl (206.5 mg, 0.551 mmol) in CD_2Cl_2 (5 mL each) were combined with stirring. After 10 minutes the solvent was removed under vacuum. The residue was suspended in toluene and transferred to a frit with a layer of silica. After filtration the solid was extracted with more toluene until the filtrate remained colorless. The combined solutions were concentrated to a volume of less than 5 mL and left for crystallization at −30 °C to give **4ad** (163.9 mg, 73%) as yellow crystals. $C_{22}H_{36}B_2CoCl$ (416.5) calcd. C 63.44, H 8.71; found C 63.30, H 8.52. ^{1}H NMR (250 MHz, $CDCl_3$): δ = 0.96 (d, ^3J = 7.3 Hz, 8 Me), 1.43 (sept, ^3J = 7.3 Hz, 4 BCH), 5.52 (m, 2 2-/5-H), 5.54 (m, 2 3-/4-H) ppm. ^{11}B{^{1}H} NMR (160 MHz, CD_2Cl_2): δ = 36.9 ppm. ^{13}C{^{1}H} NMR (63 MHz, $CDCl_3$): δ = 20.02 (Me), 22.0 (br., BCH), 85.12 (C-3,4), 88.24 (C-2,5) ppm.

Co[C_5H_4(BMe$_2$)][C_5H_4(BMe$_2$Cl)] (4bd): A preparation as described for (**1a**)Cl from (**1b**)$AlCl_4$ [1] (437.4 mg, 1.00 mmol) and PPh_4Cl (368.3 mg, 0.98 mmol) gave **4bd** (299.0 mg, 100%) as a yellow powder which was crystallized from Et_2O/CD_2Cl_2 at −30 °C; m.p. 96 °C (dec.). [The use of (**1b**)$AlCl_4$ instead of (**1b**)PF_6 is more convenient here since (**1b**)PF_6 was made from (**1b**)$AlCl_4$ by anion metathesis.] $C_{14}H_{20}B_2ClCo$ (304.3) calcd. C 55.26, H 6.62; found C 54.68, H 6.84. SIMS (DTE/DTT/Sul): positive ions *m*/*z* (%) = 269 (100) [M^+ − Cl], 229 (16) [CoCp{C_5H_4(BMe$_2$)}$^+$]. ^{1}H NMR (500 MHz, CD_2Cl_2, room temp.): δ = 0.54 (s, 4 Me), 5.48 (m, 2 2-/5-H), 5.51 (m, N = 3.7 Hz, 2 3-/4-H) ppm; the assignment for the ring protons is based on ^{1}H{^{1}H}NOE difference spectra. ^{11}B{^{1}H} NMR (160 MHz, CD_2Cl_2, room temp.): δ = 36.8 ppm. ^{13}C{^{1}H} NMR (126 MHz, CD_2Cl_2, room temp.): δ = 13.0 (br., Me), 85.69 (C-3,4), 87.94 (C-2,5) ppm; the assignment for the ring-carbon nuclei is based on heteronuclear correlation spectra or (^{1}H, ^{13}C) HMQC spectra.

Variable Temperature NMR Spectra of 4bd in CD_2Cl_2: ^{1}H and ^{13}C{^{1}H} NMR spectra of **4bd** in CD_2Cl_2 show decoalescence and the presence of two species at low temperatures (Scheme 5). Both species display effective C_{2v} symmetry, but their constitutions could be assigned by means of systematic comparisons of the chemical shifts observed for various species **4**; note especially the large difference of chemical shifts for the B-Me groups [δ = 0.60 ppm for **4bd-B** and δ = −0.15 ppmfor **4bd-C**]. The semi-quaternized isomer **4bd-B** is the major isomer and the chelate form **4bd-C** the minor isomer over the entire temperature range. The relative concentrations measured and the deduced thermodynamic parameters are collected in Table 1. Rate constants for the ring-opening reaction were obtained from line-shape analyses for the spectra of the minor isomer. The ^{1}H signals of the B-Me groups and the ^{13}C{^{1}H} signals of the carbon atoms C-2,5 and C-3,4 were suitable; the remaining signals were not used because the coupling constants of the ring

Table 1. Equilibrium data for **4bd** (see Scheme 5)

T (K)	K	$\Delta_R G$ (kJ·mol^{-1})
173	15.1	−3.90
183	16.5	−4.27
193	17.7	−4.61
203	19.8	−5.03
$\Delta_R H$ = (2.6 ± 1.1) kJ·mol^{-1}		
$\Delta_R S$ = (37.6 ± 5.4) J·K^{-1}·mol^{-1}		

protons are not easily accessible with the necessary precision and because the carbon atoms attached to boron are quadrupole-broadened. Rate constants for the ring-closure reaction were calculated using the equation $k_{-1} = K/k$. The resulting activation parameters in terms of the Eyring equation are collected in Table 2.

Table 2. Kinetic data and activation parameters for **4bd**

T (K)	K	k_1 (s^{-1})	K_{-1} (s^{-1})
193	17.7	15	0.85
203	19.8	70	3.54
213	21.2	250	11.79
243	25.4	2600	102.36
For the ring opening:		$\Delta H^{\neq}_1 = (38.0 \pm 3.0)$ kJ·mol^{-1}	
		$\Delta S^{\neq}_1 = (-18 \pm 13)$ J·K^{-1}·mol^{-1}	
For the ring closure:		$\Delta H^{\neq}_{-1} = (35.2 \pm 3.0)$ kJ·mol^{-1}	
		$\Delta S^{\neq}_{-1} = (-56 \pm 13)$ J·K^{-1}·mol^{-1}	

Data for 4bd-B: C_s symmetry, 94.7% at −90 °C. ^{1}H NMR (500 MHz, CD_2Cl_2, −90 °C): δ = 0.60 (s, 4 Me), 5.56 (s, 2 C_5H_4) ppm. $^{13}C\{^1H\}$ NMR (126 MHz, CD_2Cl_2, −90 °C): δ = 12.9 (br., Me), 86.28 (C-3,4), 87.77 (C-2,5) ppm.
Data for 4bd-C: C_{2v} symmetry, 5.3% at −90 °C. ^{1}H NMR (500 MHz, CD_2Cl_2, −90 °C): δ = −0.15 (s, 4 Me), 5.26 (s, 2 C_5H_4) ppm. $^{13}C\{^1H\}$ NMR (126 MHz, CD_2Cl_2, −90 °C): δ = 10.6 (br., Me), 83.20 (C-3,4), 86.99 (C-2,5) ppm.

Co[C_5H_4(B*i*Pr$_2$)][C_5H_4(B*i*Pr$_2$Br)] (4ae) and Co[C_5H_4(B*i*Pr$_2$)][C_5H_4(B*i*Pr$_2$I)] (4af): These compounds were prepared as described for **4ac** and **4ad** with PPh_4Br and PPh_4I, respectively. $^{11}B\{^1H\}$ NMR (160 MHz, CD_2Cl_2): δ = 43.8 for **4ae** and δ = 48.5 ppm for **4af**.

Co[C_5H_4(B*i*Pr$_2$)]$_2$(μ-OH) (4ab): Freshly powdered KOH (25.6 mg, 0.46 mmol) was added to (**1a**)PF_6 (253.1 mg, 0.48 mmol) in CH_2Cl_2 (15 mL). The suspension was then stirred for 1 d. Workup as described for **4ac** gave **4ab** (124.3 mg, 69%) as a brownish yellow solid. ^{1}H NMR (500 MHz, CD_2Cl_2): δ = 0.86 (s, 4 Me + 4 BCH), 1.01 (br. d, ^3J = 5.8 Hz, 4 Me), 2.37 (s, OH), 5.19 (m, 2 2-/5-H), 5.24 (m, 2 3-/4-H) ppm. $^{11}B\{^1H\}$ NMR (160 MHz, CD_2Cl_2): δ = 1.4 ppm. $^{13}C\{^1H\}$ NMR (126 MHz, CD_2Cl_2): δ = 21.48 and 22.28 (Me), 22.1 (br., BCH), 82.81 (C-3,4), 88.04 (C-2,5) ppm.

Co[C_5H_4(BMe$_2$)]$_2$(μ-OH) (4bb): Preparation from powdered KOH (27.3 mg, 0.49 mmol) and (**1b**)PF_6 (212.0 mg, 0.51 mmol) in nitromethane instead of CH_2Cl_2 gave **4bb** (128.6 mg, 92%) as an orange microcrystalline solid; m.p. 125 °C. $C_{14}H_{21}B_2CoO$ (285.9) calcd. C 58.82, H 7.40; found C 58.82, H 7.41. SIMS (DTE/DTT/Sul): positive ions m/z (%) = 269 (100) [M^+ − OH]. ^{1}H NMR (500 MHz, CD_2Cl_2): δ = −0.12 (s, 4 Me), 1.95 (s, OH), 5.17 (m, $N \approx$ 3.8 Hz, 2 2-/5-H), 5.24 (m, 2 3-/4-H) ppm. $^{11}B\{^1H\}$ NMR (160 MHz, CD_2Cl_2): δ = −1.9 ppm. $^{13}C\{^1H\}$ NMR (126 MHz, CD_2Cl_2): δ = 10.8 (br., Me), 82.71 (C-3,4), 87.30 (C-2,5) ppm.

Co[C_5H_4(B*i*Pr$_2$)]$_2$(μ-NH$_2$) (4aa): A solution of (**1a**)PF_6 (641.4 mg, 1.22 mmol) in CH_2Cl_2 (20 mL) was added to solid sodium amide (254.8 mg, 6.53 mmol). The resulting suspension was stirred for 7 d. The solvent was then removed under vacuum. The residue was suspended in toluene and filtered through silica. Removal of the solvent left **4aa** (434.0 mg, 90%) as a brown-orange solid which was recrystallized from toluene at −30 °C; m.p. 152 °C. $C_{22}H_{38}B_2CoN$ (397.1) calcd. C 66.54, H 9.65, N 3.53. SIMS (K/T): positive ions m/z (%) = 396 (2) [M^+ − H], 354 (100) [M^+ − *i*Pr], 228 (19) [M^+ − *i*Pr − $2C_3H_6$]; negative ions m/z (%) = 397 (100) [M^-], 354 (22) [M^- − *i*Pr], 161 (6) [C_5H_4B*i*Pr$_2^-$]. ^{1}H NMR (250 MHz, CD_2Cl_2): δ = 0.86 (overlapping, 4 BCH), 0.88 (d, J = 5.5 Hz, 4 Me), 0.96 (d, J = 6.2 Hz, 4 Me), 2.19 (br. s, NH_2), 5.15 (m, 2 2-/5-H), 5.17 (m, 2 3-/4-H) ppm; coupling constants in C_6D_6 solution: N = 3.7 Hz for C_5H_4 part and $^3J \approx$ 7.2 Hz for *i*Pr groups. $^{11}B\{^1H\}$ NMR (160 MHz, C_6D_6): δ = −8.5 ppm. $^{13}C\{^1H\}$ NMR (63 MHz, CD_2Cl_2): δ = 22.20 and 22.97 (Me), 82.23 (C-3,4), 87.59 (C-2,5) ppm.

NMe$_4$[Co{C_5H_4(B*i*Pr$_2$F)}$_2$] (5): A solution of (**1a**)PF_6 (456.6 mg, 0.868 mmol) in CH_2Cl_2 (10 mL) was added to solid NMe_4F (172.4 mg, 1.851 mmol). After stirring for 3 h all volatiles were removed under vacuum. The residue was suspended in toluene and filtered through a frit. The remaining solid was intensively washed with more toluene. The combined filtrates were liberated from solvent to give **5** (380 mg, 89%) as orange microcrystals; m.p. 160 °C (dec.). $C_{26}H_{48}B_2CoF_2N$ (493.2) calcd. C 63.31, H 9.81, N 2.84; found C 63.44, H 10.01, N 2.91. SIMS (K/T): positive ions m/z (%) = 74 (100) [NMe_4^+]; negative ions m/z (%) = 419 (100) [M^- − NMe_4], 400 (10) [419 − F], 376 (23) [419 − C_3H_7], 333 (7) [Co(C_5H_4B*i*PrF)$_2^-$]. ^{1}H NMR (500 MHz, CD_2Cl_2): δ = 0.62 (sept, 4 BCH), 0.71 and 0.75 (d, ^3J = 7.0 Hz, 4 Me each), 3.36 (s, NMe_4), 5.05 (m, 2 2-/5-H), 5.16 (br. m, N = 3.7 Hz, 2 3-/4-H) ppm. $^{11}B\{^1H\}$ NMR (160 MHz, CD_2Cl_2): δ = 3.4 (d, $^1J_{F,B}$ = 61 Hz) ppm. $^{13}C\{^1H\}$ NMR (126 MHz, CD_2Cl_2): δ = 21.14 and 21.21 (d, $^3J_{F,C}$ = 5.5 Hz, Me), 21.6 (br., BCH), 56.41 (t, $^1J_{N,C}$ = 3.8 Hz, NMe_4), 80.70 (C-3,4), 85.29 (d, $^3J_{F,C}$ = 5.5 Hz, C-2,5) ppm. ^{19}F NMR (470 MHz, C_6D_6): δ = −194 ($\nu_{1/2}$ = 153 Hz) ppm.

K[Co{C_5H_4(B*i*Pr$_2$OH)}$_2$] (6): Freshly powdered KOH (24.5 mg, 0.44 mmol) was added to a solution of **4ab** (135.2 mg, 0.34 mmol) in THF (10 mL). After stirring the suspension for 24 h it was filtered through silica. The volatiles were removed from the orange filtrate under vacuum. The resulting brown oil was dissolved in toluene (3 mL) and diluted with hexane (10 mL). After standing for several days at room temperature brownish yellow needles of **6** (67.7 mg, 44%) had formed; m.p. > 210 °C. $C_{22}H_{38}B_2CoKO_2$ (454.2) calcd. C 58.18, H 8.43; found C 58.04, H 8.53. SIMS (K/T): negative ions m/z (%) = 471 (100) [M + OH^-]; positive ions m/z (%) = 303 (100) [K^+ + [18]-crown-6]. ^{1}H NMR (500 MHz, [D_8]THF): δ = 0.07 (br. s, 2 OH), 0.54 (sept, 4 BCH), 0.69 and 0.73 and (d, ^3J = 7.1 Hz, 4 Me each), 5.09 (m, 2 × 2-/5-H), 5.11 (m, 2 × 3-/4-H) ppm. $^{11}B\{^1H\}$ NMR (160 MHz, [D_8]THF): δ = −3.1 ppm. $^{13}C\{^1H\}$ NMR (126 MHz, [D_8]THF): δ = 21.40 and 21. 76 (Me), 22.7 (br., BCH), 80.19 (C-3,4), 86.10 (C-2,5) ppm.

X-ray Crystal Structure Determinations: Geometry and intensity data were collected with ENRAF-Nonius CAD4 diffractometers (Mo-K_α radiation with graphite monochromators). Crystal data, data-collection parameters, and convergence results for the compounds (**1b**)PF_6, **4bd**, **4ac**, and **5** are listed in Table 3. The structures of (**1b**)PF_6, **4bd**, and **5** were solved by direct methods[26a] and subsequent Fourier difference syntheses, whereas the coordinates of the corresponding hydroxo compound **4ab** provided the structure model for **4ac**. In the full-matrix least-squares refinements on intensities[26b] non-hydrogen atoms were assigned anisotropic displacement parameters and hydrogen atoms were included with standard geometry. The refinement of **4ac** deserves a comment: This compound is isomorphous with the hydroxide **4ab** with similar, but significantly different, lattice parameters. Refinement of the chelated anion site with the scattering factor for *F* results in clearly superior reliability factors than a model for chelated hydroxide. The best results were obtained when a mixed occupancy of the anion site was refined; convergence was reached for an approximate F:O ratio of 4:1, in good agreement with spectroscopic evidence. CCDC-232238 for (**1b**)PF_6, -232239 for **4bd**, -232240 for **4ac**, and -232241 for **5** contain the supplementary crystallographic data of

Table 3. Crystal data, data collection parameters, and convergence results for (**1b**)PF_6, **4bd**, **4ac** and **5**

	(**1b**)PF_6	**4bd**	**4ac**	**5**
Empirical formula	$C_{14}H_{20}B_2CoF_6P$	$C_{14}H_{20}B_2ClCo$	$C_{22}H_{36.2}B_2CoF_{0.8}O_{0.2}$	$C_{26}H_{48}B_2CoF_2N$
Molecular mass	413.82	304.30	399.66	493.20
Crystal system	monoclinic	triclinic	orthorhombic	monoclinic
Space group	$P2_1/m$ (11)	$P\bar{1}$ (2)	$Pccn$ (56)	$C2/c$ (15)
Radiation (λ, Å)	Mo-K_α (0.71073)	Mo-K_α (0.71073)	Mo-K_α (0.71073)	Mo-K_α (0.71073)
a (Å)	8.040(2)	8.153(3)	7.8665(9)	15.2028(12)
b (Å)	12.574(3)	9.390(2)	14.3884(18)	7.7185(4)
c (Å)	8.612(2)	10.373(3)	18.710(2)	25.2446(11)
α (°)		94.01(2)		
β (°)	100.95(2)	92.37(2)		102.574(5)
γ (°)		113.490(18)		
V (Å^3)	854.8(4)	724.4(4)	2117.7(4)	2891.2(3)
Z	2	2	4	4
$d_{calcd.}$ (g/cm^3)	1.608	1.395	1.254	1.133
F(000)	420	316	856	1064
μ (mm^{-1})	1.150	1.346	0.821	4.845
Absorption correction	numerical	numerical	none	empirical
Max./min. transmission	0.877/0.758	0.721/0.640		0.530/0.377
θ range (°)	3−28	3−26	2−28	6−74
Temperature (K)	203	203	203	293
Scan mode	ω	ω−2θ	ω−2θ	ω−2θ
Crystal size (mm)	0.45 × 0.24 × 0.12	0.70 × 0.40 × 0.26	0.2 × 0.2 × 0.2	0.25 × 0.15 × 0.15
Reflections collected	5136	3086	5300	4925
Reflections unique	1841	2837	2559	2898
Refls. observed $I > 2\sigma(I)$	1443	2615	1130	1488
Variables	138	328	120	177
R_1[a] observed (all data)	0.0519 (0.0730)	0.0275 (0.0315)	0.0620 (0.1696)	0.0471 (0.1483)
wR_2[b] observed (all data)	0.1406 (0.1494)	0.0746 (0.0761)	0.0860 (0.0975)	0.1066 (0.1215)
GOF[c]	1.077	1.059	0.958	0.925
Max. resd. density (e/Å^3)	0.962	0.357	0.659	0.190

[a] $R_1 = \|F_o| - |F_c\|/|F_o|$. [b] $wR_2 = [w(F_o^2 - F_c^2)^2/w(F_o^2)^2]^{1/2}$, where $w = 1/[\sigma^2(F_o^2) + (aP)^2]$ and $P = [\max(F_o^2,0) + 2F_c^2]/3$. [c] GOF = $[w(F_o^2 - F_c^2)^2/(n - p)]^{1/2}$.

this paper. These data can be obtained free of charge at www.ccdc.cam.ac.uk/conts/retrieving/html or from the Cambridge Crystallographic Data Centre, 12 Union Road, Cambridge CB2 1EZ, UK [Fax: (internat.) + 44-1223-336-033; E-mail: deposit@ccdc.cam.ac.uk].

Acknowledgments

This work was generously supported by the Deutsche Forschungsgemeinschaft and the Fonds der Chemischen Industrie.

[1] G. E. Herberich, U. Englert, A. Fischer, D. Wiebelhaus, *Organometallics* **1998**, *17*, 4769−4775.
[2] D. Wiebelhaus, Dissertation, Technische Hochschule Aachen, Aachen, Germany, **1998**.
[3] [3a] J.-M. Lehn, *Supramolecular Chemistry*, VCH, Weinheim, **1995**. [3b] F. Vögtle, *Supramolecular Chemistry*, John Wiley & Sons, Chichester, England, **1993**. [3c] *Molecular Recognition* (Ed.: S. H. Gellman), Thematic issue of *Chem. Rev.* (July/August), **1997**.
[4] [4a] C. Suksai, T. Tuntulani, *Chem. Soc. Rev.* **2003**, *32*, 192−202. [4b] P. D. Beer, P. A. Gale, *Angew. Chem.* **2001**, *113*, 502−532; *Angew. Chem. Int. Ed.* **2001**, *40*, 486−516. [4c] F. P. Schmidtchen, M. Berger, *Chem. Rev.* **1997**, *97*, 1609−1646. [4d] *The Supramolecular Chemistry of Anions* (Eds.: A. Bianchi, K. Bowman-James, E. Garcia-España), Wiley-VCH, Weinheim, **1997**.
[5] [5a] M. J. Biallas, D. F. Shriver, *J. Am. Chem. Soc.* **1966**, *88*, 375−376. [5b] D. F. Shriver, M. J. Biallas, *J. Am. Chem. Soc.* **1967**, *89*, 1078−1081. [5c] M. J. Biallas, *J. Am. Chem. Soc.* **1969**, *91*, 7290−7292.
[6] [6a] H. E. Katz, *J. Am. Chem. Soc.* **1985**, *107*, 1420−1421. [6b] H. E. Katz, *J. Org. Chem.* **1985**, *50*, 5027−5032. [6c] H. E. Katz, *Organometallics* **1987**, *6*, 1134−1136.
[7] D. H. Busch, *Chem. Rev.* **1993**, *93*, 847−860.
[8] [8a] D. J. Saturnino, M. Yamauchi, W. R. Clayton, R. W. Nelson, S. G. Shore, *J. Am. Chem. Soc.* **1975**, *97*, 6063−6070. [8b] R. Köster, G. Seidel, *Chem. Ber.* **1992**, *125*, 627−636. [8c] R. Köster, G. Seidel, K. Wagner, B. Wrackmeyer, *Chem. Ber.* **1993**, *126*, 305−317.
[9] V. C. Williams, G. J. Irvine, W. E. Piers, Z. Li, S. Collins, W. Clegg, M. R. J. Elsegood, T. B. Marder, *Organometallics* **2000**, *19*, 1619−1621.
[10] G. E. Herberich, A. Fischer, D. Wiebelhaus, *Organometallics* **1996**, *15*, 3106−3108.
[11] G. E. Herberich, A. Fischer, *Organometallics* **1996**, *15*, 58−67.
[12] [12a] N. G. Connelly, W. E. Geiger, *Chem. Rev.* **1996**, *96*, 877−910. [12b] A. N. Nesmeyanov, R. B. Materikova, I. R. Lyatifov, T. K. Kurbanov, N. S. Kochetkova, *J. Organomet. Chem.* **1978**, *145*, 241−243.
[13] J. F. Klang, D. B. Collum, *Organometallics* **1988**, *7*, 1532−1537.
[14] For reference data see: [14a] H. Nöth, B. Wrackmeyer, in *NMR Basic Principles and Progress* (Eds.: P. Diehl, E. Fluck, R. Kosfeld), Springer Verlag, Berlin, **1978**, vol. 14. [14b]B. Wrackmeyer, *Annu. Rep. NMR Spectrosc.* **1988**, *20*, 61−203. [14c] A. R. Siedle, *Annu. Rep. NMR Spectrosc.* **1988**, *20*, 205−314.

[15] A. L. Spek, *Acta Crystallogr., Sect. A* **1990**, *46*, C34.
[16] The acronym *cog* denotes the center of gravity of the C5 ring.
[17] [17a] C. K. Narula, H. Nöth, *Inorg. Chem.* **1985**, *24*, 2532−2539. [17b] T. Wagner, U. Eigendorf, G. E. Herberich, U. Englert, *Struct. Chem.* **1994**, *5*, 233−237.
[18] F. H. Allen, O. Kennard, D. G. Watson, L. Brammer, A. G. Orpen, R. Tylor, *J. Chem. Soc., Perkin Trans. 2* **1987**, S1−S19.
[19] [19a] T. D. Coyle, F. G. A. Stone, in *Progress in Boron Chemistry* (Eds.: H. Steinberg, A. L. McCoskey), Pergamon Press, Oxford, **1964**, vol. 1, 83−166. [19b]D. Mootz, M. Steffen, *Z. Anorg. Allg. Chem.* **1981**, *483*, 171−1180. [19c] D. J. Brauer, H. Bürger, G. Pawelke, *Inorg. Chem.* **1977**, *16*, 2305−2314. [19d] D. J. Brauer, H. Bürger, G. Pawelke, *J. Organomet. Chem.* **1980**, *192*, 305−317. [19e] D. J. Brauer, H. Bürger, G. Pawelke, *J. Organomet. Chem.* **1982**, *238*, 267−279. [19f] M. J. R. Clark, H. Lynton, *Can. J. Chem.* **1970**, *48*, 405−409.
[20] F. H. Allen, *Acta Crystallogr., Sect. B* **2002**, *58*, 380−388.
[21] *X-Blackboard*, Version 2.3.8; number of records searched, April 2003: 272066 (no disorder, coordinates available, error-free, $R < 0.1$).
[22] P. Braunstein, L. Douce, J. Fischer, N. C. Craig, G. Goetz-Grandmont, D. Matt, *Inorg. Chim. Acta* **1992**, *194*, 151−156.
[23] R. Köster, W. Schüßler, R. Boese, *Chem. Ber.* **1990**, *123*, 1945−1952.
[24] R. Fuhler, T. Lenzen, G. Hägele, *Comp. Chem.* **1995**, *19*, 277−282.
[25] J. Sandström, *Dynamic NMR Spectroscopy*, Academic Press, London, England, **1982**.
[26] [26a] G. M. Sheldrick, *SHELXS-97: Program for Structure Solution*; University of Göttingen, Göttingen, Germany, **1997**. [26b] G. M. Sheldrick, *SHELXL-97: Program for Structure Refinement*; University of Göttingen, Göttingen, Germany, **1997**.

Received April 2, 2004
Early View Article
Published Online August 12, 2004

